TWO-PHASE FLOW HEAT TRANSFER MEASUREMENTS AND CORRELATION FOR THE ENTIRE FLOW MAP IN HORIZONTAL PIPES

A Ghajar, J Kim, and C Tang
School of Mechanical and Aerospace Engineering, Oklahoma State University, Stillwater, OK 74078, USA

Abstract

Local heat transfer coefficients and flow parameters were measured for air-water flow in a pipe in the horizontal position and all the flow patterns in the entire flow map. The test section was a 27.9 mm stainless steel pipe with a length to diameter ratio of 100. A total of 179 heat transfer data points were taken on horizontal position by carefully coordinating the liquid and gas superficial Reynolds number combinations. The heat transfer data were measured under a uniform wall heat flux boundary condition ranging from about 3000 W/m^2 to 10,800 W/m^2. The superficial Reynolds numbers ranged from about 740 to 26,000 for water and from about 700 to 48,000 for air. These experimental data including all the flow patterns in the entire flow map were reasonably well correlated by a general two-phase heat transfer correlation with 75% of the data predicted within ±20% deviation, and 86% of them were within ±30% deviation. The validation with the experimental data confirmed the robustness of the general two-phase heat transfer correlation to adequately predict the experimental data for most of the flow patterns and wide ranges of the superficial liquid and gas Reynolds numbers ($700 < Re_{SL} < 26{,}000$ and $700 < Re_{SG} < 48{,}000$).

Nomenclature

C	leading coefficient, dimensionless
D	inside diameter of a circular tube, m
F_P	flow pattern factor, dimensionless
F_S	shape factor, dimensionless
h_L	heat transfer coefficient as if liquid alone were flowing, W/m^2·K
h_{TP}	overall mean two-phase heat transfer coefficient, W/m^2·K
k	thermal conductivity, W/m·K
K	slip ratio, dimensionless
m	constant exponent value on the quality ratio term, dimensionless
$\dot{m}$	mass flow rate, kg/s or kg/min
n	constant exponent value on the void fraction ratio, dimensionless
Pr	Prandtl number, dimensionless
p	constant exponent value on the Prandtl number ratio term, dimensionless
q	constant exponent value on the viscosity ratio term, dimensionless
Re_L	liquid in-situ Reynolds number, dimensionless
Re_{SG}	superficial gas Reynolds number, dimensionless
Re_{SL}	superficial liquid Reynolds number, dimensionless
S_L	wetted-perimeter, m
u	axial velocity, m/s
x	quality, dimensionless

Greek Symbols

α	void fraction, dimensionless
μ	dynamic viscosity, Pa·s
ρ	density, kg/m^3

Subscripts

B	bulk
CAL	calculated
eff	effective
eq	equilibrium
EXP	experimental
G	gas phase
L	liquid phase
m	mixture
W	wall

Superscript

~	non-dimensionalized

1. Introduction

Gas-liquid two-phase flow in pipes is commonly observed in industrial applications, such as oil wells and pipelines. Due to changing conditions, liquid hydrocarbons produced from many oil and gas reservoirs can become unstable while being transported through pipelines and begin to crystallize and deposit on the walls of the pipelines. The hydrodynamic and thermal conditions of two-phase flow are dependent upon the interaction between the two phases. However, due to the complex nature of the two-phase gas-liquid flow, the accessible heat transfer data and applicable correlations for non-boiling two-phase flow in horizontal and inclined pipes covering various flow patterns and inclined positions are limited in the literature. Most of the available heat transfer correlations are often limited by specific flow pattern or flow orientation. A comprehensive discussion of the available experimental data and heat transfer correlations for forced convective heat transfer during gas-liquid two-phase flow in vertical and horizontal pipes, including flow patterns and fluid combinations is provided by Kim et al. (1999). Kim and Ghajar (2006) developed a general overall heat transfer coefficient correlation for non-boiling gas-liquid two-phase flow with different flow patterns in horizontal pipes. However, the validation of the general heat transfer correlation was limited to plug, slug, slug/bubbly, slug/bubbly/annular, and annular flow patterns only.

The objectives of this study were to extend the knowledge base by gathering quality non-boiling, two-phase, two-component heat transfer data in the horizontal position with all the flow patterns of the entire flow map, and analyze their behavior and extend the capability of a general overall heat transfer coefficient correlation which was developed by our research team, see Kim et al. (2000) and Kim and Ghajar (2006). In order to achieve this goal, the nature of the heat transfer in air-water two-phase flow was investigated by comparing the two-phase heat transfer data that were obtained by systematically varying the air or water flow rates (flow pattern).

2. Development of Heat Transfer Correlation

In order to predict the heat transfer coefficient in two-phase flow, regardless of flow pattern, Kim and Ghajar (2006) developed a new correlation based on the work of Kim et al. (2000). The correlation developed by Kim et al. (2000) has been successfully applied to the experimental data taken in our laboratory [Kim and Ghajar (2002), Ghajar (2004), and Ghajar et al. (2004a,b,c)]. However, the weighting factor (void fraction) used in our correlation does not fully account for the effect of different flow patterns on the two-phase heat transfer data. In the past we had to use different set of constants for different flow patterns (Kim and Ghajar, 2002). Therefore, in order to handle the effect of various flow patterns on the two-phase heat transfer data with only one correlation, the flow pattern factor (F_P) was developed.

The void fraction (α) which is the volume fraction of the gas-phase in the tube cross-sectional area, does not reflect the actual wetted-perimeter (S_L) in the tube with respect to the corresponding flow pattern. For instance, in the case of a plug flow the void fraction is near zero while the non-dimensionalized wetted-perimeter is near unity, but in the case of an annular flow the void fraction and the wetted-perimeter both approach unity. However, the estimation of the actual wetted-perimeter is very difficult due to the continuous interaction of the two phases in the tube. Therefore, instead of estimating the actual wetted-perimeter, modeling the effective wetted-perimeter is a more practical approach. In our model we have ignored the influence of the surface tension and the contact angle of each phase on the effective wetted-perimeter.

As shown in Figure 1, the shape of the gas-liquid interface at the equilibrium state (see Figure 1a) based on the void fraction (α) is far different from the realistic case (see Figure 1b). As mentioned before, the two-phase heat transfer correlation weighted by the void fraction is not capable of

distinguishing the differences between the different flow patterns. Therefore, in order to capture the realistic shape of the gas-liquid interface, the flow pattern factor (F_P), an effective wetted-perimeter relation is proposed:

$$F_P = \tilde{S}^2_{L,eff} = \left(\frac{S_{L,eff}}{\pi D}\right)^2 = (1-\alpha) + \alpha F_S^2 . \tag{1}$$

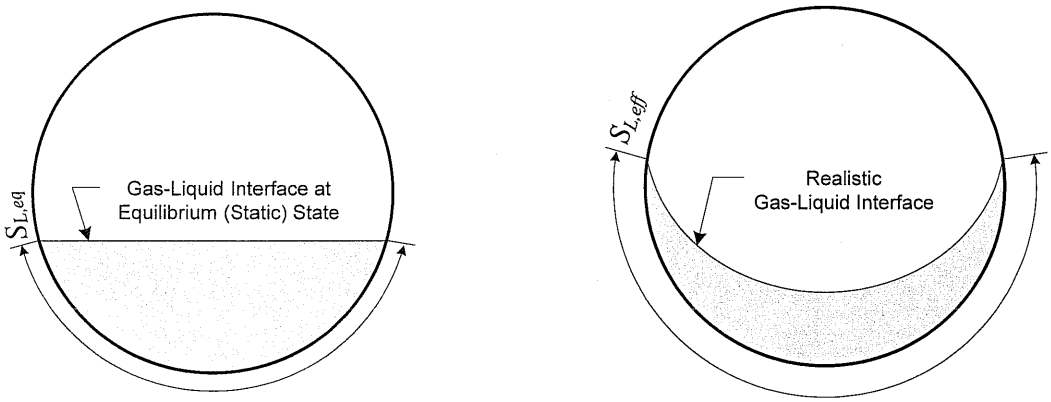

(a) equilibrium state (b) realistic (effective) interface

Figure 1. Gas-liquid interfaces and wetted-perimeters.

The term F_S appearing in equation (1) is referred to as shape factor which in essence is a modified and normalized Froude number. The shape factor (F_S) is defined as:

$$F_S = \frac{2}{\pi}\tan^{-1}\left(\sqrt{\frac{\rho_G (u_G - u_L)^2}{g D(\rho_L - \rho_G)}}\right). \tag{2}$$

The shape factor (F_S) is applicable for slip ratio $K(=u_G/u_L)\geq 1$, which is common in gas-liquid flow, and represents the shape changes of the gas-liquid interface by the force acting on the interface due to the relative momentum and gravity forces.

With the introduction of the flow pattern factor (F_P), the heat transfer correlation takes the following form [see Kim and Ghajar (2006)]:

$$h_{TP} = F_P\, h_L \left\{1 + C\left[\left(\frac{x}{1-x}\right)^m \left(\frac{1-F_P}{F_P}\right)^n \left(\frac{Pr_G}{Pr_L}\right)^p \left(\frac{\mu_G}{\mu_L}\right)^q\right]\right\}, \tag{3}$$

where h_L comes from the Sieder and Tate (1936) correlation for turbulent flow given as

$$h_L = 0.027\,\mathrm{Re}_L^{4/5}\,\mathrm{Pr}_L^{1/3}\left(\frac{k_L}{D}\right)\left(\frac{\mu_B}{\mu_W}\right)_L^{0.14}. \tag{4}$$

For the Reynolds number needed in the h_L calculation, the following relationship is used to evaluate the in-situ Reynolds number (liquid phase) rather than the superficial liquid Reynolds number (Re_{SL}) as commonly used in the correlations available in the literature [see Kim et al. (1999)]:

$$Re_L = \left(\frac{\rho u D}{\mu}\right)_L = \frac{4\dot{m}_L}{\pi\sqrt{1-\alpha}\,\mu_L D}. \quad (5)$$

The values of the void fraction (α) used in equations (1), (3) and (5) are calculated based on the correlation provided by Chisholm (1973) in this study, which can be expressed as

$$\alpha = \left[1+\left(\frac{\rho_L}{\rho_m}\right)^{1/2}\left(\frac{1-x}{x}\right)\left(\frac{\rho_G}{\rho_L}\right)\right]^{-1}, \quad (6)$$

where $1/\rho_m = (1-x)/\rho_L + x/\rho_G$ and $x = \dot{m}_G/(\dot{m}_G + \dot{m}_L)$.

Note that any other well-known correlations for single-phase turbulent heat transfer and void fraction could have been used in place of the Sieder and Tate (1936) correlation and Chisholm (1973) correlation, respectively. The difference resulting from the use of different correlations will be absorbed during the determination of the values of the leading coefficient and exponents on the different parameters in equation (3).

3. Experimental Setup

A schematic diagram of the overall experimental setup for heat transfer and pressure drop measurements and flow visualizations in two-phase air-water pipe flow in horizontal and inclined positions is shown in Figure 2. The test section is a 27.9 mm straight standard stainless steel schedule 10S pipe with a length to diameter ratio of a 100. The setup rests atop an aluminum I-beam that is supported by a pivoting foot and a stationary foot that incorporates a small electric screw jack. The I-beam is approximately 9 m in length and can be inclined to an angle of approximately 8° above horizontal.

The water flow rate was measured by a Micro Motion Coriolis flow meter (model CMF125) connected to a digital Field-Mount Transmitter (model RFT9739) that conditioned the flow information for the data acquisition system. The air flow rate was measured by a Micro Motion Coriolis flow meter (model CMF100) connected to a digital Field-Mount Transmitter (model RFT9739) and regulated by a needle valve.

T-type thermocouples were cemented with Omegabond 101, an epoxy adhesive with high thermal conductivity and electrical resistivity, to the outside wall of the stainless steel test section (refer to Figure 3). Omega EXPP-T-20-TWSH extension wires were used for relay to the data acquisition system. The thermocouples were placed on the outer surface of the tube wall at uniform intervals of 254 mm from the entrance to the exit of the test section. There were 10 thermocouple stations in the test section. All stations had four thermocouples, and they were labeled looking at the tail of the fluid flow with peripheral location "A" being at the top of the tube, "B" being 90° in the clockwise direction, "C" at the bottom of the tube, and "D" being 90° from the bottom in the clockwise sense (refer to Figure 3). The inlet liquid and gas temperatures and the exit bulk temperature were measured by Omega TMQSS-125U-6 thermocouple probes. The thermocouple probe for the exit bulk temperature was placed after the mixing well. To ensure a uniform fluid bulk temperature at the inlet and exit of the test section, a mixing well was utilized. An alternating polypropylene baffle type static mixer for both gas and liquid phases was used. This mixer provided an overlapping baffled passage forcing the fluid to encounter flow reversal and swirling regions. The mixing well at the exit of the test section was placed below the clear polycarbonate observation section (after the test section), and before the liquid storage tank (refer to Figure 2).

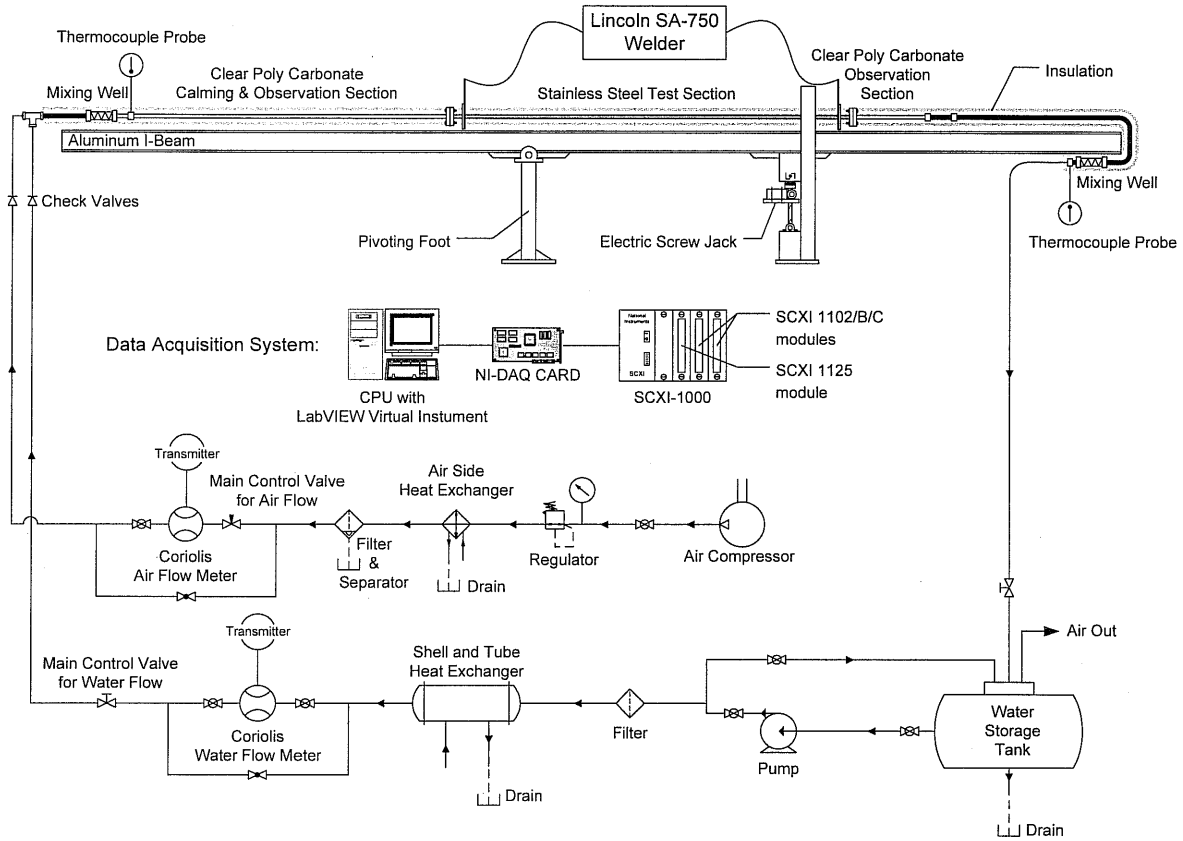

Figure 2. Schematic of experimental setup.

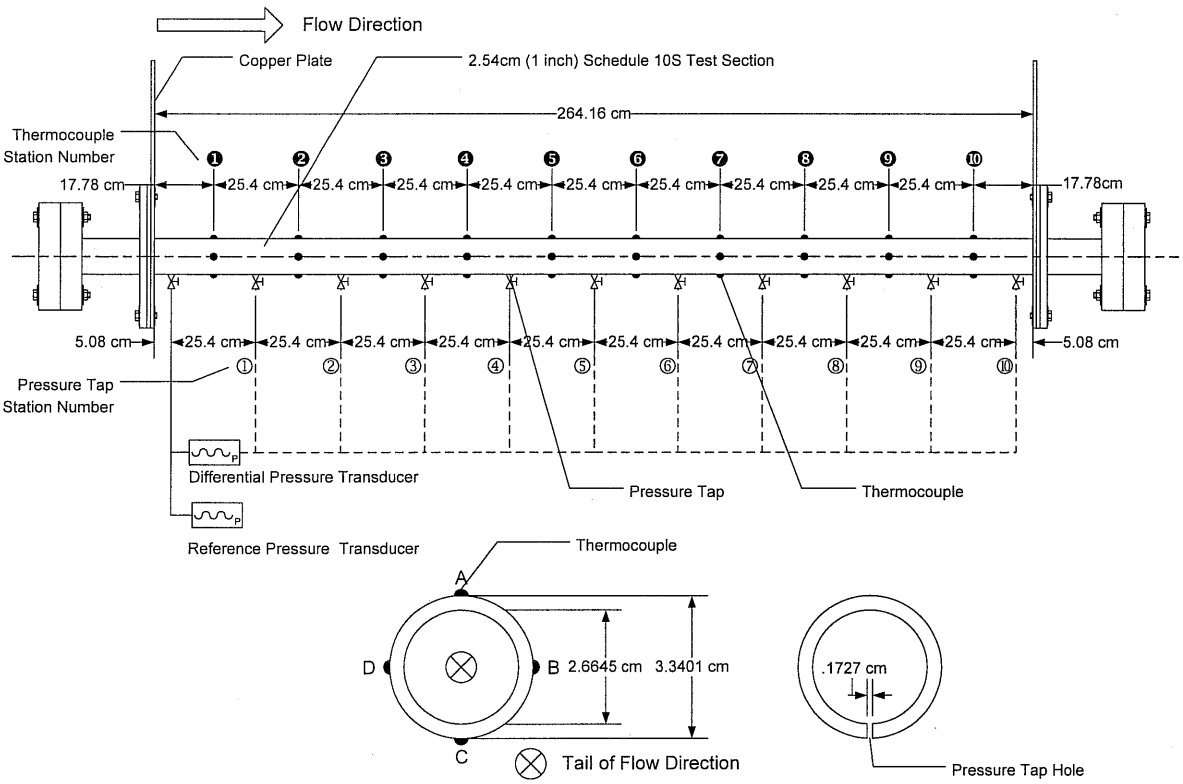

Figure 3. Test section.

The heat transfer measurements at uniform wall heat flux boundary condition were carried out by measuring the local outside wall temperatures at 10 stations along the axis of the tube and the inlet and outlet bulk temperatures in addition to other measurements such as the flow rates of gas and liquid, room temperature, voltage drop across the test section, and current carried by the test section. The peripheral heat transfer coefficient (local average) were calculated based on the knowledge of the pipe inside wall surface temperature and inside wall heat flux obtained from a data reduction program developed exclusively for this type of experiments (Ghajar and Kim, 2006). The local average peripheral values for inside wall temperature, inside wall heat flux, and heat transfer coefficient were then obtained by averaging all the appropriate individual local peripheral values at each axial location. The large variation in the circumferential wall temperature distribution, which is typical for two-phase gas-liquid flow, leads to different heat transfer coefficients depending on which circumferential wall temperature was selected for the calculations.

The uncertainty analyses of the overall experimental procedures using the method of Kline and McClintock (1953) showed that there is a maximum of 11.5% uncertainty for heat transfer coefficient calculations. Experiments under the same conditions were conducted periodically to ensure the repeatability of the results. The maximum difference between the duplicated experimental runs was within ±10%. Details of the experimental setup, calibration of experimental instruments, data collection and data reduction procedures can be found from Durant (2003).

The heat transfer data obtained with the present experimental setup were measured under a uniform wall heat flux boundary condition that ranged from 2870 to 10,790 W/m^2 and the resulting overall mean two-phase heat transfer coefficients (h_{TP}) ranged from 120 to 4379 W/m^2·K for horizontal flow. For these experiments, the liquid superficial Reynolds number (Re_{SL}) ranged from 738 to 26,053 (water mass flow rates from about 1.03 to 33.7 kg/min) and the gas superficial Reynolds numbers (Re_{SG}) ranged from 698 to 47,611 (gas mass flow rates from about 0.017 to 1.13 kg/min).

4. Results and Discussions

4.1. Flow Patterns

The various interpretations accorded to the multitude of flow patterns by different investigators are subjective; and no uniform procedure exists at present for describing and classifying them. In this study, the flow pattern identification for the experimental data was based on the procedures suggested by Taitel and Dukler (1976), and Kim and Ghajar (2002); and visual observations deemed appropriate. By fixing the water flow rates, flow patterns were observed at various air flow rates. Flow pattern data were obtained with the pipe at horizontal position for water flow rates of 0.7–50 kg/min and air flow rates of 0.01–1.2 kg/min. These experimental data were plotted and compared using their corresponding values of mass flow rates of air and water and the flow patterns. Representative digital images of each flow pattern were taken using a Nikon D50 digital camera with Nikkor 50mm f/1.8D lens.

Figure 4 shows the flow map with the representative photographs of the various flow patterns. The various flow patterns for horizontal flow depicted in Figure 4 show the capability of our experimental setup to cover multitude of flow patterns. The shaded lines represent the boundaries of the observed flow patterns, and its thickness depicts the transition between different flow patterns. Once the flow map of the flow patterns for horizontal flow was established, the heat transfer data for different flow patterns were then collected. Figure 5 shows the flow map with symbols representing the distribution of the heat transfer data that were collected systematically in our experimental setup. Heat transfer data at low air and water flow rate combinations (water flow rates of less than about 1 kg/min and air flow rates of less than about 0.1 kg/min) were not collected. At

such low water and air flow rates, there exists the possibility of local boiling or dry-out which could potentially damage the heated test section.

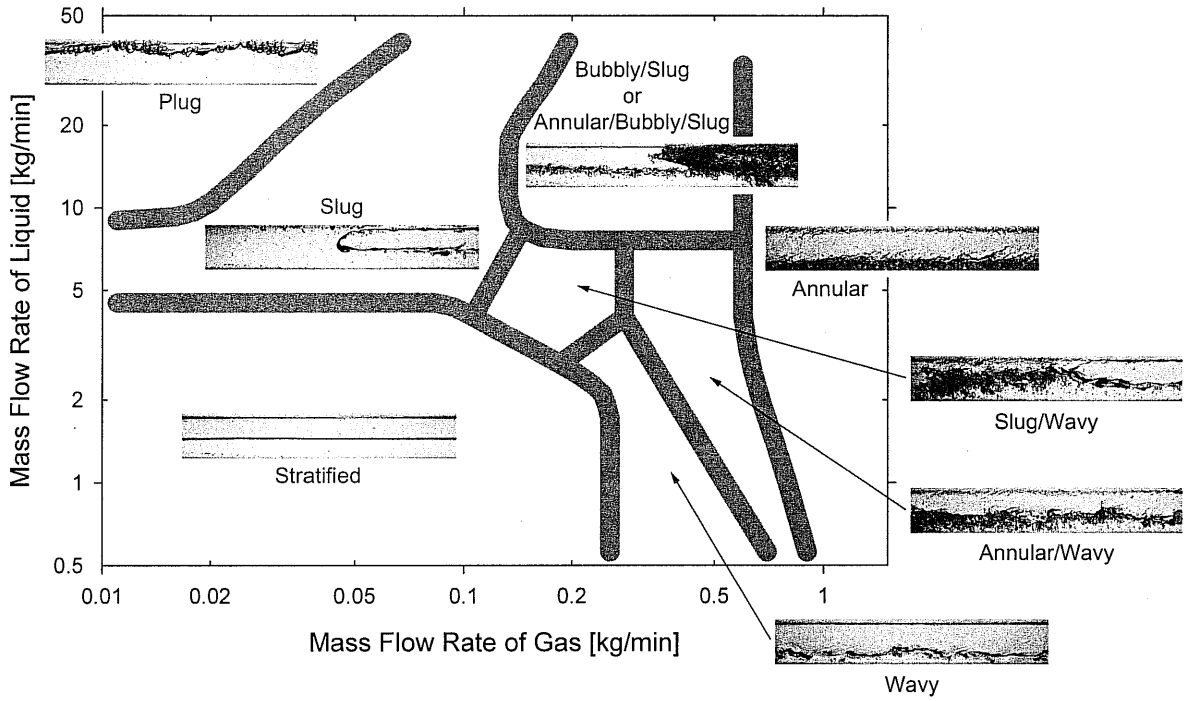

Figure 4. Flow map of horizontal flow with photographs of representative flow patterns.

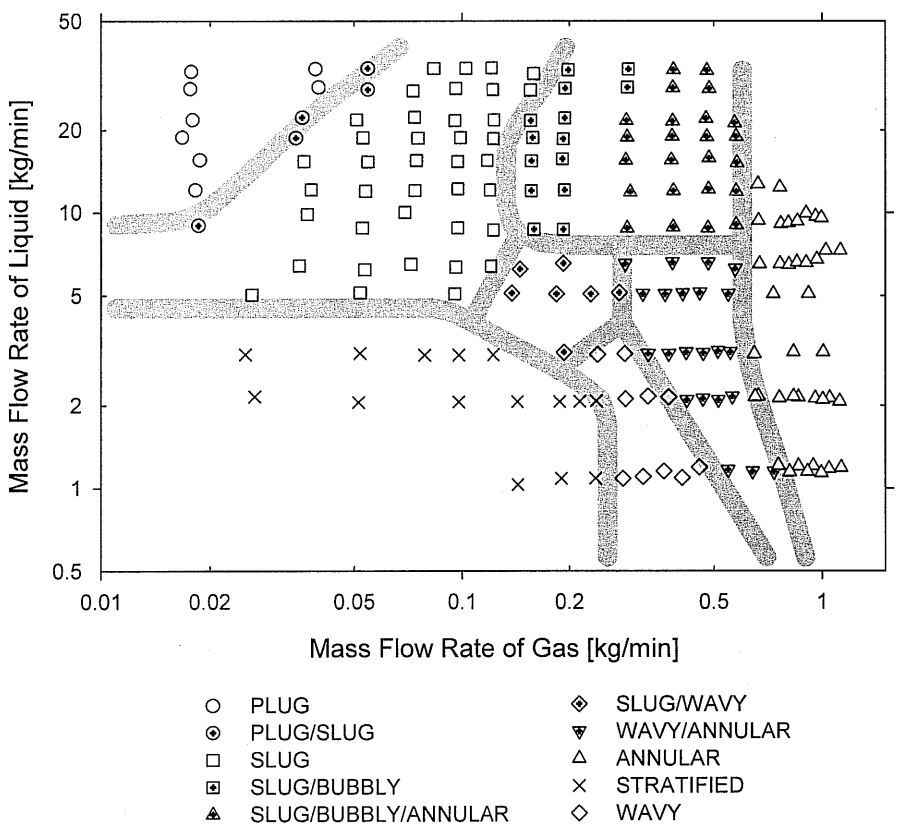

Figure 5. Flow map of horizontal flow with distribution of heat transfer data collected.

4.2. Systematic Investigation on Two-Phase Gas-Liquid Heat Transfer in Horizontal Pipe

An overview of the different trends that was observed in the heat transfer behavior of the two-phase air-water flow in horizontal pipes for a variety of flow patterns is presented here. The two-phase heat transfer data were obtained by systematically varying the air or water flow rates.

Flow pattern, superficial liquid Reynolds number (water flow rate) and superficial gas Reynolds number (air flow rate) have pronounced influence on the two-phase mean heat transfer coefficient. The results presented in Figure 6 clearly show that two-phase mean heat transfer coefficients are strongly influenced by the liquid superficial Reynolds number (Re_{SL}). As shown in Figure 6, the heat transfer coefficient increases proportionally as Re_{SL} increases. In addition, for a fixed Re_{SL}, the two-phase mean heat transfer coefficients are also influenced by the superficial gas Reynolds number (Re_{SG}) and each flow pattern shows its own distinguished heat transfer trend as shown in Figure 7. Typically, heat transfer increases at low Re_{SG} (the regime of plug flow), and then slightly decreases at the mid range of Re_{SG} (the regime of slug and slug-type transitional flows), and again increases at the high Re_{SG} (the regime of annular flow).

4.3. Validation of the Heat Transfer Correlation

Kim and Ghajar (2006) proposed a two-phase heat transfer correlation in the form given by equation (3). This correlation was designed to be capable of handling different flow patterns by means of introduction of a flow pattern factor (F_P) into the correlation. The values of the leading coefficient (C) and the exponents (m, n, p, q) in equation (3) were determined using the experimental data of Ghajar et al. (2004a,b,c).

The validation of the general heat transfer correlation, equation (3), with the then available experimental data reported by Kim and Ghajar (2006) was limited to plug, slug, slug/bubbly, slug/bubbly/annular, and annular flow patterns and liquid flow rates greater than 5 kg/min. In the current study presented here, equation (3) was further validated with a total of 179 data points for horizontal flow covering the entire flow map and all the flow patterns observable experimentally. Figure 8 shows the capability of equation (3) in predicting the experimental data. Table 1 summarizes the parameters used in the correlation and the detailed results of the predictions. Seventy five percent (75%) of the total number of experimental data were within the ±20% deviation, and 86% of them were within ±30% deviation.

Table 2 summarizes the detailed results of the predictions by the correlation equation categorized for different ranges of Re_{SL} and Re_{SG}, and all the flow patterns. The general heat transfer correlation predicted more accurately for data with Re_{SL} and Re_{SG} above 10,000; where 91% of the data with $Re_{SL} > 10{,}000$ and 89% of the data with $Re_{SG} > 10{,}000$ were predicted within the ±20% deviation. The correlation predicted the heat transfer data with reasonable accuracy for most of the flow patterns with at least 72% of the data were predicted within the ±20% deviation, except for plug flow and stratified flow. It should be noted that plug flow and stratified flow were flow patterns observed in the lower ranges of Re_{SL} and Re_{SG} (see Figure 5).

These results provide additional validation on the robustness of the two-phase heat transfer correlation to adequately predict the experimental data for majority of the flow patterns and wide ranges of Re_{SL} and Re_{SG} ($700 < Re_{SL} < 26{,}000$ and $700 < Re_{SG} < 48{,}000$). The results presented in this section clearly show that the flow pattern factor (F_P) does a very good job of accounting for the majority of the flow patterns encountered in two-phase flow in horizontal pipes with the exception of plug and stratified flows. We will focus part of our future efforts in collecting more reliable data in these flow patterns and modifying our proposed flow pattern factor to do a much better job of predicting heat transfer for these flows.

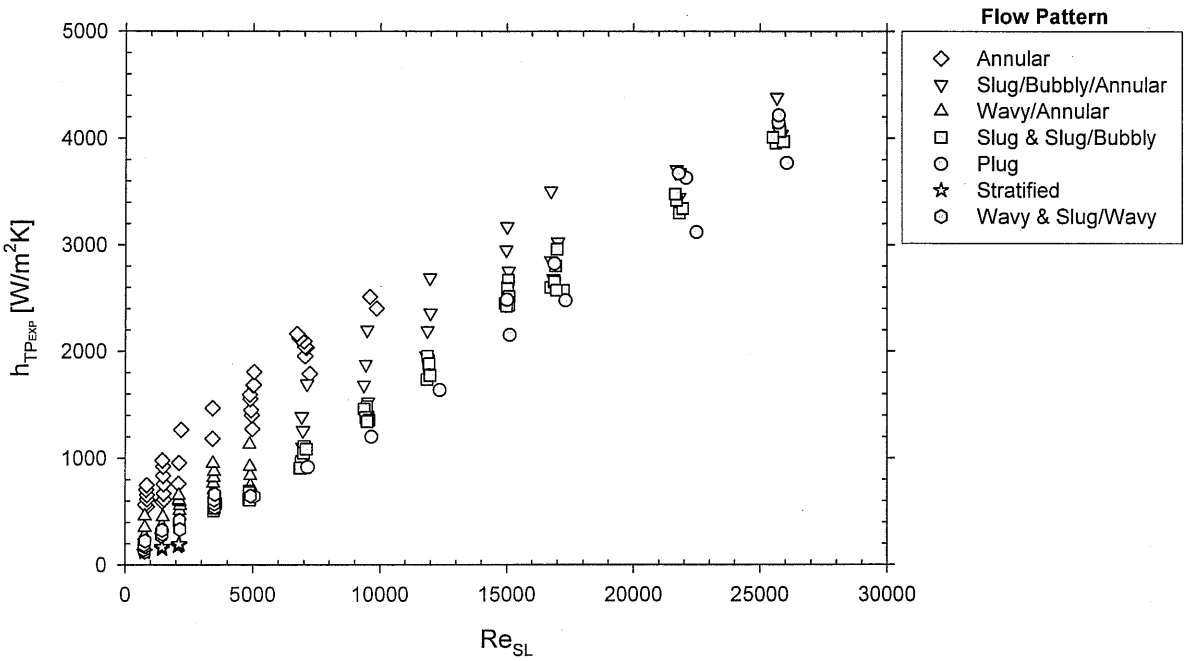

Figure 6. Variation of two-phase heat transfer coefficients with superficial liquid Reynolds number.

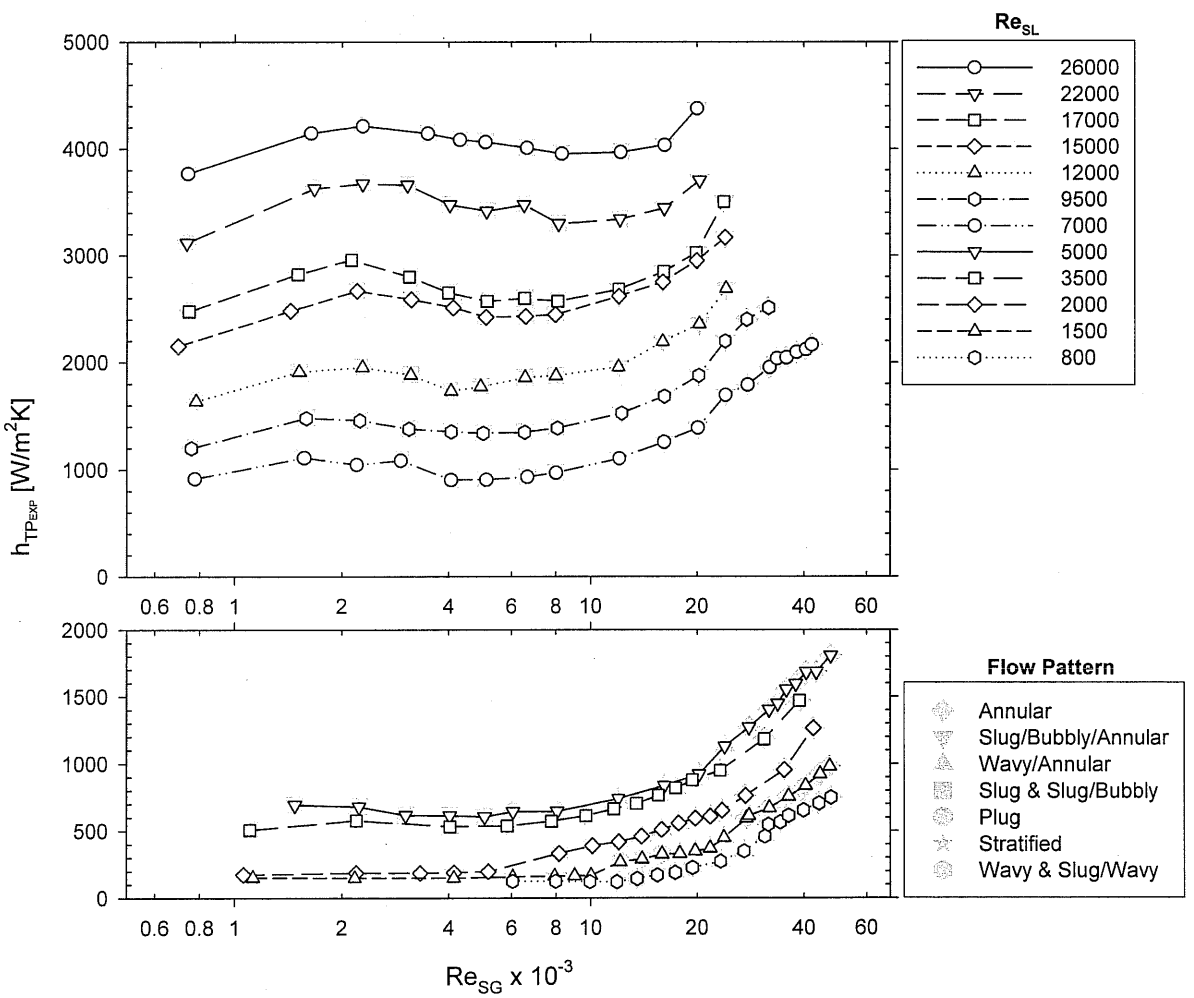

Figure 7. Variation of two-phase heat transfer coefficients with superficial gas Reynolds number.

Table 1. Determined constants, results of predictions of the horizontal air-water flow experimental data, and the parameter range for equation (3).

Exp. Data (No. of Data)	Value of C and Exponents (m, n, p, q)					Mean Dev. [%]	Std. Dev. [%]	No. of Data within ±20%	No. of Data within ±30%	Range of Parameter				
	C	m	n	p	q					Re_{SL}	F_P	x	$\left(\frac{Pr_G}{Pr_L}\right)$	$\left(\frac{\mu_G}{\mu_L}\right)$
179	0.7	0.08	0.06	0.03	-0.14	13.4	35.2	135 (75%)	154 (86%)	738 to 26054	0.109 to 0.766	5.42×10^{-4} to 0.487	0.086 to 0.110	0.015 to 0.020

Table 2. Results of predictions by equation (3) categorized for different ranges of superficial Reynolds numbers and flow patterns.

	Exp. Data (No. of Data)	Mean Dev. [%]	Std. Dev. [%]	No. of Data within ±20%	No. of Data within ±30%
$Re_{SL} < 10{,}000$	121	18.5	40.7	82 (68%)	82 (68%)
$Re_{SL} > 10{,}000$	58	2.57	15.0	53 (91%)	53 (91%)
$Re_{SG} < 10{,}000$	84	30.0	43.6	50 (60%)	61 (73%)
$Re_{SG} > 10{,}000$	95	-1.39	14.7	85 (89%)	93 (98%)
Annular	35	2.90	15.1	28 (80%)	35 (100%)
Slug/Bubbly & Slug/Bubbly/Annular	38	-5.10	7.32	38 (100%)	38 (100%)
Wavy/Annular	22	-6.82	12.2	21 (95%)	22 (100%)
Wavy & Slug/Wavy	17	9.99	11.6	13 (76%)	16 (94 %)
Slug	39	14.2	16.3	28 (72%)	34 (87%)
Plug	13	31.5	22.0	6 (46%)	6 (46%)
Stratified	15	100	58.7	1 (6.7%)	3 (20%)

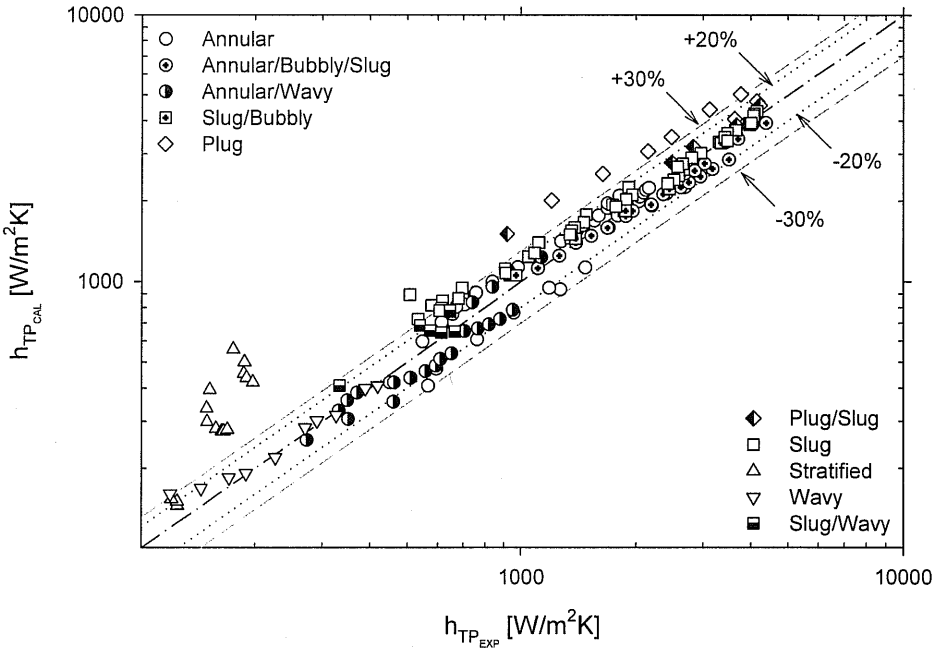

Figure 8. Comparison of the predictions of the recommended heat transfer correlation with the heat transfer data.

5. Conclusions

The purpose of this study was to further develop the knowledge and understanding of heat transfer in non-boiling two-phase, two-component flow. For this purpose air-water flow heat transfer experiments were conducted in a circular pipe in the horizontal position under uniform wall heat flux boundary condition. In the case of heat transfer in horizontal flow, the heat transfer rate proportionally increased as Re_{SL} increased. However, in more detail, it is observed that heat transfer shows distinguished trends depending on the flow pattern and Re_{SG}. Validation of the general overall heat transfer coefficient correlation for gas-liquid two-phase flow regardless of flow pattern confirmed the robustness of the correlation equation. The general heat transfer correlation was able to adequately predict experimental data for all the flow patterns in the entire flow map over wide ranges of superficial Reynolds numbers ($700 < Re_{SL} < 26{,}000$ and $700 < Re_{SG} < 48{,}000$), with 75% of the data within ±20% deviation and 86% of the data within ±30% deviation.

Acknowledgments

The authors gratefully acknowledge the financial support provided by the Oklahoma State University (OSU) Foundation and Micro Motion, Omega, Dell Computers, and National Instruments for their generous contributions and consideration to the modernization of the laboratory. The assistance of Mr. Wendell Cook (M.S. candidate) with the flow visualization part of this study is greatly appreciated.

References

Chisholm, D., 1973, Two-Phase Flow in Pipelines and Heat Exchangers, George Godwin, London and New York in association with the Institution of Chemical Engineers, New York.

Durant, W. B., 2003, Heat Transfer Measurement of Annular Two-Phase Flow in Horizontal and a Slightly Upward Inclined Tube, M.S. Thesis, Oklahoma State University, Stillwater, OK.

Ghajar, A. J., 2004, Non-Boiling Heat Transfer in Gas-Liquid Flow in Pipes — a Tutorial, ENCIT2004: Proc. of the 10th Brazilian Congress of Thermal Sciences and Engineering, Nov. 29-Dec. 3, Rio de Janeiro, Brazil.

Ghajar, A. J. and Kim, J., 2006, Calculation of Local Inside-Wall Convective Heat Transfer Parameters from Measurements of the Local Outside-Wall Temperatures along an Electrically Heated Circular Tube: Chapter 23 in Heat Transfer Calculations, edited by M. Kutz, McGraw-Hill, New York, pp. 23.3–23.27.

Ghajar, A. J., Kim, J., Durant, W. B., and Trimble, S. A., 2004a, An Experimental Study of Heat Transfer in Annular Two-Phase Flow in A Horizontal and Slightly Upward Inclined Tube, HEFAT2004: Proc. 3rd International Conference on Heat Transfer, Fluid Mechanics and Thermodynamics, June 21-24, Cape Town, South Africa, Paper No. GA1.

Ghajar, A. J., Kim, J., Malhotra, K., and Trimble, S. A., 2004b, Systematic Heat Transfer Measurements for Air-Water Two-Phase Flow in a Horizontal and Slightly Upward Inclined Pipe, ENCIT2004: Proc. of the 10th Brazilian Congress of Thermal Sciences and Engineering, Nov. 29-Dec. 3, Rio de Janeiro, Brazil, Paper No. CIT04-0471.

Ghajar, A. J., Malhotra, K., Kim, J., and Trimble, S. A., 2004c, Heat Transfer Measurements and Correlations for Air-Water Two-Phase Slug Flow in a Horizontal Pipe, HT-FED2004: Proc. of 2004 ASME Heat Transfer/Fluids Engineering Summer Conference, July 11-15, Charlotte, North Carolina, Paper No. HT-FED2004-56614.

Kim, D. and Ghajar, A. J., 2002, Heat Transfer Measurements and Correlations for Air-Water Flow of Different Flow Patterns in a Horizontal Pipe, Experimental Thermal and Fluid Science, 25, pp. 659–676.

Kim, J. and Ghajar, A. J., 2006, A General Heat Transfer Correlation for Non-Boiling Gas-Liquid Flow with Different Flow Patterns in Horizontal Pipes, International Journal of Multiphase Flow, 32(4), pp. 447-465.

Kim D., Ghajar A. J., and Dougherty R. L., 2000, Robust Heat Transfer Correlation for Turbulent Gas-Liquid Flow in Vertical Pipes, J. Thermophysics and Heat Transfer, 14(4), pp. 574–578.

Kim, D., Ghajar, A. J., Dougherty, R. L., and Ryali, V. K., 1999, Comparison of 20 Two-Phase Heat Transfer Correlations with Seven Sets of Experimental Data, Including Flow Pattern and Tube Inclination Effects, Heat Transfer Engineering, 20(1), pp. 15–40.

Kline, S. J. and McClintock, F. A., 1953, Describing Uncertainties in Single-Sample Experiments, Mech. Engr., 1, pp. 3–8.

Sieder, E. N. and Tate, G. E., 1936, Heat Transfer and Pressure Drop of Liquids in Tubes, Industrial & Engineering Chemistry, 28(12), pp. 1429–1435.

Taitel, Y and Dukler, A.E., 1976, Model for Predicting Flow Regime Transitions in Horizontal and Near Horizontal Gas-Liquid Flow, AIChE Journal, 22(1), pp. 47–55.